A Combined Theoretical−Experimental Study of the Inclusion of Niobocene Dichloride in Native and Permethylated β-Cyclodextrins

Cláudia C. L. Pereira, Mariela Nolasco, Susana S. Braga, Filipe A. Almeida Paz, Paulo Ribeiro-Claro, Martyn Pillinger, and Isabel S. Gonçalves*

Department of Chemistry, CICECO, University of Aveiro, 3810-193 Aveiro, Portugal

Received April 16, 2007

Inclusion complexes comprising niobocene dichloride, Cp_2NbCl_2, and either native β-cyclodextrin (β-CD) or permethylated β-CD (TRIMEB) were prepared with a host:guest molar ratio of 1:1. The adducts were characterized in the solid state by powder X-ray diffraction (XRD), thermogravimetric analysis (TGA), $^{13}C\{^1H\}$ CP/MAS NMR, FTIR, and FT Raman spectroscopies. Ab initio calculations were performed in order to elucidate the possible inclusion geometries and calculate vibrational frequencies for Cp_2NbCl_2 in the region 100−1800 cm^{-1}. The vibrational spectra indicated that neither the hosts nor the guest were chemically modified upon inclusion complexation. Small wavenumber shifts in C−H, C−C, and metal−ligand vibrational modes were attributed to the effect of the host−guest interaction. Powder XRD showed that the β-CD adduct was of low crystallinity, while the TRIMEB adduct was quite crystalline. The powder XRD pattern of the TRIMEB adduct could be satisfactorily indexed in the monoclinic system with the space group $P2_1$. A hypothetical structural model for the crystal packing was obtained through Monte Carlo optimizations using a reported TRIMEB geometry comprising a distorted elliptical cavity. An unrestrained Rietveld refinement of the structural model could not be carried out due to the relatively low quality of the experimental powder XRD pattern. However, the plausibility of the host−guest interaction geometry, involving inclusion of one of the guest Cp ligands inside the CD cavity, was fully supported by the ab initio calculations.

Introduction

Cyclodextrins (CDs) are cyclic oligosaccharides comprising six (α-CD), seven (β-CD), eight (γ-CD), or more D-glucose units linked by α-(1→4) glycosidic bonds.[1−3] Their shape is like a hollow truncated cone, and they have no hydroxy groups inside their cavity. Although the depths of the cavities for the three CD molecules are the same (7.9 Å), their diameters are different: ca. 5.7, 7.8, and 9.5 Å for α-, β-, and γ-CD, respectively. This internal cavity, which is highly hydrophobic, can accommodate a wide range of guest molecules, ranging from polar compounds such as alcohols, acids, amines, and small inorganic anions to apolar compounds such as aliphatic and aromatic hydrocarbons.[3−5] CDs function as second-sphere ligands toward many transition metal complexes and organometallic compounds,[6] such as diammine(1,1-cyclobutanedicar-

* To whom correspondence should be addressed. E-mail: igoncalves@dq.ua.pt.

(1) Harata, K. In *Comprehensive Supramolecular Chemistry*; Szejtli, J., Osa, T., Eds.; Pergamon: Oxford, 1996; Vol. 3, pp 279−304.
(2) Saenger, W.; Steiner, T. *Acta Crystallogr.* **1998**, *A54*, 798.
(3) Szejtli, J. *Chem. Rev.* **1998**, *98*, 1743.
(4) Saenger, W. *Angew. Chem., Int. Ed. Engl.* **1980**, *19*, 344.
(5) Fenyvesi, E.; Szente, L.; Russel, N. R.; McNamara, M. In *Comprehensive Supramolecular Chemistry*; Szejtli, J., Osa, T., Eds.; Pergamon: Oxford, 1996; Vol. 3, pp 305−366.
(6) (a) Hapiot, F.; Tilloy, S.; Monflier, E. *Chem. Rev.* **2006**, *106*, 767. (b) Sliwa, W.; Girek, T. *Heterocycles* **2003**, *60*, 2147.
(7) Alston, D. R.; Ashton, P. R.; Lilley, T. H.; Stoddart, J. F.; Zarzycki, R.; Slawin, A. M. Z.; Williams, D. J. *Carbohydr. Res.* **1989**, *192*, 259.
(8) (a) Breslow, R.; Trainor, G.; Ueno, A. *J. Am. Chem. Soc.* **1983**, *105*, 2739. (b) Matsue, T.; Evans, D. H.; Osa, T.; Kobayashi, N. *J. Am. Chem. Soc.* **1985**, *107*, 3411. (c) Harada, A.; Takahashi, S. *J. Chem. Soc., Chem. Commun.* **1984**, 645. (d) Harada, A.; Hu, Y.; Yamamoto, S.; Takahashi, S. *J. Chem. Soc., Dalton Trans.* **1988**, 729. (e) Odagaki, Y.; Hirotsu, K.; Higuchi, T.; Harada, A.; Takahashi, S. *J. Chem. Soc., Perkin Trans.* **1990**, *1*, 1230. (f) Liu, Y.; Zhong, R.-Q.; Zhang, H.-Y.; Song, H.-B. *Chem. Commun.* **2005**, 2211. (g) Ju, H.; Leech, D. *Langmuir* **1998**, *14*, 300. (h) Kaifer, A. E. *Acc. Chem. Res.* **1999**, *32*, 62. (i) Coutouli-Argyropoulou, E.; Kelaidopoulou, A.; Sideris, C.; Kokkinidis, G. *J. Electroanal. Chem.* **1999**, *477*, 130. (j) Osella, D.; Carretta, A.; Nervi, C.; Ravera, M.; Gobetto, R. *Organometallics* **2000**, *19*, 2791. (k) Fernandes, J. A.; Lima, S.; Braga, S. S.; Ribeiro-Claro, P.; Rodriguez-Borges, J. E.; Teixeira, C.; Pillinger, M.; Teixeira-Dias, J. J. C.; Gonçalves, I. S. *J. Organomet. Chem.* **2005**, *690*, 4801. (l) Fernandes, J. A.; Lima, S.; Braga, S. S.; Pillinger, M.; Rodríguez-Borges, J. E.; Ribeiro-Claro, P.; Teixeira-Dias, J. J. C.; Gonçalves, I. S. *Eur. J. Inorg. Chem.* **2005**, 4729. (m) Fernandes, J. A.; Lima, S.; Braga, S. S.; Pillinger, M.; Ribeiro-Claro, P.; Rodriguez-Borges, J. E.; Lopes, A. D.; Teixeira-Dias, J. J. C.; Gonçalves, I. S. *Organometallics* **2005**, *24*, 5673.
(9) (a) Turel, I.; Demšar, A.; Košmrlj, J. *J. Inclusion Phenom. Macrocyclic Chem.* **1999**, *35*, 595. (b) Vinklárek, J.; Honzíček, J.; Holubová, J. *Central Eur. J. Chem.* **2005**, *3*, 72. (c) Braga, S. S.; Gonçalves, I. S.; Pillinger, M.; Ribeiro-Claro, P.; Teixeira-Dias, J. J. C. *J. Organomet. Chem.* **2001**, *632*, 11. (d) Braga, S. S.; Marques, M. P. M.; Sousa, J. B.; Pillinger, M.; Teixeira-Dias, J. J. C.; Gonçalves, I. S. *J. Organomet. Chem.* **2005**, *690*, 2905.
(10) Meister, G.; Stoeckli-Evans, H.; Süss-Fink, G. *J. Organomet. Chem.* **1993**, *453*, 249.
(11) Klingert, B.; Rihs, G. *J. Chem. Soc., Dalton Trans.* **1991**, 2749.
(12) (a) Shimada, M.; Harada, A.; Takahashi, S. *J. Chem. Soc., Chem. Commun.* **1991**, 263. (b) Patel, P. P.; Welker, M. E. *J. Organomet. Chem.* **1997**, *547*, 103. (c) Díaz, C.; Arancibia, A. *J. Inclusion Phenom. Macrocyclic Chem.* **1998**, *30*, 127. (d) Braga, S. S.; Gonçalves, I. S.; Ribeiro-Claro, P.; Lopes, A. D.; Pillinger, M.; Teixeira-Dias, J. J. C.; Rocha, J.; Romão, C. C. *Supramol. Chem.* **2002**, *14*, 359. (e) Braga, S. S.; Almeida Paz, F. A.; Pillinger, M.; Seixas, J. D.; Romão, C. C.; Gonçalves, I. S. *Eur. J. Inorg. Chem.* **2006**, 1662. (f) Alston, D. R.; Slawin, A. M. Z.; Stoddart, J. F.; Williams, D. J. *Angew. Chem., Int. Ed. Engl.* **1985**, *24*, 786. (g) Song, L.; Meng, Q.; You, X. *J. Organomet. Chem.* **1995**, *498*, C1. (h) Harada, A.; Saeki, K.; Takahashi, S. *Organometallics* **1989**, *8*, 730. (i) Braga, S. S.; Gago, S.; Seixas, J. D.; Valente, A. A.; Pillinger, M.; Santos, T. M.; Gonçalves, I. S.; Romão, C. C. *Inorg. Chim. Acta* **2006**, *359*, 4757. (j) Braga, S. S.; Gonçalves, I. S.; Lopes, A. D.; Pillinger, M.; Rocha, J.; Romão, C. C.; Teixeira-Dias, J. J. C. *J. Chem. Soc., Dalton Trans.* **2000**, 2964. (k) Lima, S.; Gonçalves, I. S.; Ribeiro-Claro, P.; Pillinger, M.; Lopes, A. D.; Ferreira, P.; Teixeira-Dias, J. J. C.; Rocha, J.; Romão, C. C. *Organometallics* **2001**, *20*, 2191. (l) Pereira, C. C. L.; Braga, S. S.; Almeida Paz, F. A.; Pillinger, M.; Klinowski, J.; Gonçalves, I. S. *Eur. J. Inorg. Chem.* **2006**, 4278.

10.1021/om7003749 CCC: $37.00
Publication on Web 07/12/2007

boxylato)platinum(II) (carboplatin),[7] ferrocene and its derivatives,[8] metallocene dihalides,[9] aromatic ruthenium complexes,[10] mixed sandwich complexes such as $[(\eta^5\text{-}C_5H_5)Fe(\eta^6\text{-}C_6H_6)](PF_6)$,[11] and numerous half-sandwich metal carbonyl and cyano complexes.[12] The driving forces for the inclusion complexation of CDs with these types of guests are attributed to several factors such as van der Waals forces, hydrophobic interactions, electronic effects, and steric factors. Encapsulated metallo-organic complexes often exhibit markedly different physical and chemical characteristics compared to the bulk material.

The bioorganometallic chemistry of many of the metal complexes referred to above is of particular interest, especially in relation to their use as pharmaceuticals.[13] However, poor aqueous solubility and stability are common drawbacks of metal-based drug molecules. The encapsulation of these molecules in cyclodextrins is one method that has the potential to improve their physicochemical characteristics and bioavailabilities, as well as reducing toxic side effects.[14] With respect to metallocene dichlorides Cp_2MCl_2, which are of considerable interest as anticancer agents,[15] studies have been have been carried out with M = Ti, V, and Mo. From solution NMR studies, Turel et al. assumed that the hydrolysis products $[Cp_2Ti(H_2O)(Cl)]^+$ and $[Cp_2Ti(H_2O)_2]^{2+}$ were the species incorporated in β-CD and γ-CD cavities.[9a] Unfortunately, the degree of complexation in the isolated solid-state products could not be determined. We were able to isolate a stoichiometric well-defined crystalline material through the treatment of β-CD with aqueous Cp_2MoCl_2.[9c] The evidence suggested that Cp_2MoCl_2 was the species incorporated in the CD cavity rather than $[Cp_2Mo(H_2O)Cl]^+$ or $[Cp_2Mo(H_2O)_2]^{2+}$. Cytotoxicity experiments carried out on human adenocarcinoma cells indicated that the antitumor activity of Cp_2MoCl_2 can be enhanced by association with cyclodextrins, in particular the modified cyclodextrin heptakis-2,3,6-tri-*O*-methyl-β-CD (TRIMEB).[9d]

The difficulty in obtaining high-quality single crystals suitable for X-ray diffraction (XRD) has meant that only a few solid-state structures have been fully determined for CD inclusion compounds containing metallo-organic complexes. Nevertheless, full characterization using other methods such as powder XRD and NMR can provide important structural information.[12e,16] Molecular modeling calculations also help to investigate host−guest interactions and predict possible binding modes.[8k−m,9c,17] Herein, we describe a combined theoretical (ab initio calculations)−experimental (powder XRD, TGA, solid-state NMR, and vibrational spectroscopy) study of the encapsulation of Cp_2NbCl_2 in β-CD and permethylated β-CD (TRIMEB).

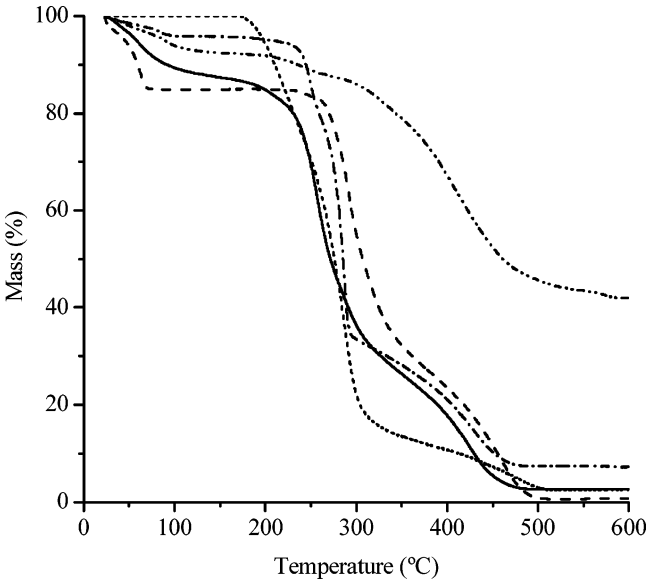

Figure 1. Thermogravimetric profiles of Cp_2NbCl_2 (− · · − · ·), native β-CD hydrate (− − − −), the β-CD inclusion complex **2** (—), TRIMEB (- - -), and the TRIMEB inclusion complex **3** (− · − · −).

Results and Discussion

The relative solubilities of the hosts β-CD and TRIMEB determined the method used for the preparation of the respective inclusion complexes. A CD/Cp_2NbCl_2 molar ratio of 1:1 was used for both systems. The β-CD inclusion complex was prepared by adding a solution of β-CD in water to a cold solution of Cp_2NbCl_2 (**1**) in dry ethanol. A pale yellow solid, designated as β-CD·Cp_2NbCl_2·$10H_2O$ (**2**), was obtained after evaporation of the solvent. Inclusion in TRIMEB was achieved by dropwise addition of a solution of TRIMEB in undried dichloromethane to a solution of **1** in dry ethanol. After stirring for 20 min in an ice bath, the solvent was evaporated, giving the complex TRIMEB·Cp_2NbCl_2·$4H_2O$ (**3**) as a pale greenish-yellow solid. The absence of significant amounts of residual organic solvent(s) in the two inclusion complexes was confirmed by the solid-state $^{13}C\{^1H\}$ CP/MAS NMR spectra, while the presence of water was indicated by the TGA curves (see below). Complexes **2** and **3** are soluble in ethanol and acetonitrile. The color of complex **2** is an indication that at least partial oxidation of the metal to a Nb^V complex occurred during the inclusion process.[18]

Figure 1 shows the thermogravimetric traces of Cp_2NbCl_2, native β-CD hydrate, TRIMEB, and the two inclusion complexes. Niobocene dichloride decomposes in the temperature range 200−600 °C, leaving a residual mass of 42%. TGA of β-CD shows a well-defined weight loss of 15% from room temperature up to 75 °C, assigned to removal of water molecules located in the β-CD cavities and also in the interstices between the macrocycles (ca. 11 water molecules per β-CD molecule). The corresponding dehydration profile for β-CD·Cp_2NbCl_2·$10H_2O$ (**2**) is different and extends over a wider range, with a weight loss of 12.0% at 130 °C. Native β-CD hydrate starts to melt and decompose at about 250 °C, and two steps are observed up to 500 °C, at which point the mass loss is 100%. The degradation of the inclusion complex is similar, except that the first step is shifted to lower temperature by about 35 °C and the final residual mass at 490 °C is 2.7%. The lower temperature

(13) *Bioorganometallics: Biomolecules, Labeling, Medicine*; Jaouen, G., Ed.; Wiley-VCH: Weinheim, Germany, 2005.

(14) (a) Davis, M. E.; Brewster, M. E. *Nat. Rev. Drug Discovery* **2004**, *3*, 1023. (b) Challa, R.; Ahuja, A.; Ali, J.; Khar, R. K. *AAPS PharmSciTech.* **2005**, *6*, E329. (c) Utsuki, T.; Brem, H.; Pitha, J.; Loftsson, T.; Kristmundsdottir, T.; Tyler, B. M.; Olivi, A. *J. Controlled Release* **1996**, *40*, 251. (d) Burgos, A. E.; Belchior, J. C.; Sinisterra, R. D. *Biomaterials* **2002**, *23*, 2519.

(15) (a) Harding, M. M.; Mokdsi, G. *Curr. Med. Chem.* **2000**, *7*, 1289. (b) Vinklárek, J.; Paláčková, H.; Honzíček, J.; Holubová, J.; Holčapek, M.; Císařová, I. *Inorg. Chem.* **2006**, *45*, 2156, and references therein.

(16) (a) Caira, M. R. *Rev. Roum. Chim.* **2001**, *46*, 371. (b) Schneider, H.-J.; Hacket, F.; Rüdiger, V. *Chem. Rev.* **1998**, *98*, 1755. (c) Caron, L.; Christine, C.; Tilloy, S.; Monflier, E.; Landy, D.; Fourmentin, S.; Surpateanu, G. *Supramol. Chem.* **2002**, *14*, 11.

(17) (a) Lipkowitz, K. B. *Chem. Rev.* **1998**, *98*, 1829. (b) Bonnet, P.; Jaime, C.; Morin-Allory, L. *J. Org. Chem.* **2002**, *67*, 8602. (c) Bonnet, P.; Beà, I.; Jaime, C.; Morin-Allory, L. *Supramol. Chem.* **2003**, *15*, 251. (d) Alcaro, S.; Battaglia, D.; Ortuso, F. *ARKIVOC* **2004**, Part (v), 107. (e) Faucci, M. T.; Melani, F.; Mura, P. *Chem. Phys. Lett.* **2002**, *358*, 383. (f) Varady, J.; Wu, X.; Wang, S. *J. Phys. Chem. B* **2002**, *106*, 4863. (g) Granados, A. M.; de Rossi, R. H.; Barbiric, D. J.; Castro, E. A. *J. Mol. Struct. (THEOCHEM)* **2002**, *619*, 91.

(18) Harding, M. M.; Prodigalidad, M.; Lynch, M. J. *J. Med. Chem.* **1996**, *39*, 5012.

degradation of the host relative to native β-CD hydrate [or a physical mixture of the two components in a 1:1 molar ratio (not shown)] can be ascribed to the promoting effect of niobium on the decomposition of the organic macrocycle. This is evidence for the existence of a significant host−guest interaction in the inclusion complex.[12h,j] The TRIMEB inclusion complex **3** exhibits a somewhat different TG behavior. After removal of water molecules from room temperature to 95 °C (4% mass loss), the onset of decomposition is around 230 °C, which is 55 °C higher than that observed for pure TRIMEB [and 30 °C higher than that observed for a physical mixture of the two components in a 1:1 molar ratio (not shown)]. The higher stability of the inclusion complex must be related with the different conformation of the macrocycle and/or its packing arrangement in the solid state. A similar result was obtained for the TRIMEB inclusion complex of Cp_2MoCl_2.[9d] As seen for complex **2**, the decomposition of **3** occurs essentially in two main steps up to about 500 °C and leaves a residual mass of 7.4%.

Powder XRD showed that complex **2** was of low crystallinity, exhibiting only a few broad and weak reflections (not shown). The absence of peaks characteristic of either crystalline Cp_2NbCl_2 or native β-CD hydrate was an initial indication for the formation of a true inclusion complex, although the type of crystal-packing arrangement could not be determined. In contrast to complex **2**, the TRIMEB adduct **3** is quite crystalline, which allowed the nature of the crystal-packing arrangement to be assessed by means of a direct comparison between the experimental powder XRD pattern and those typically observed for inclusion complexes of TRIMEB with organic guests.[8k,12e,16a,19] In the earlier report by M. R. Caira,[16a] an isostructural series for TRIMEB inclusion complexes with organic guests was identified, in which all of the complexes crystallized in the orthorhombic crystal system with space group $P2_12_12_1$. Attempts to index the collected powder XRD pattern of the inclusion complex **3** by means of the routines provided with the software program DICVOL04,[20] and constraining the variables in order to maintain the typical orthorhombic unit cell parameters described by Caira, failed to produce chemically reasonable metrics. A Le Bail[21] whole-powder-diffraction-pattern profile fitting in $P2_12_12_1$ using typical orthorhombic unit cell parameters was unsuccessful in producing sensible refinements. These did not converge and were systematically characterized by large fitting errors (for example, $R_{Bragg} = 1.33\%$ and $\chi^2 = 33.8$; see Figure S1 in the Supporting Information).

A systematic search in a more recent compilation of the Cambridge Structural Database (CSD, Version 5.27, November 2005)[22] than that used by Caira revealed 32 entries for inclusion complexes containing TRIMEB, all with organic guests.[23] Six of these structures were fully described in the monoclinic crystal system,[24] all in the $P2_1$ space group with approximately half the volume of the more common orthorhombic unit cell. Taking this into account, the experimental powder XRD pattern of TRIMEB·Cp_2NbCl_2·$4H_2O$ (**3**) was indexed using DICVOL04, by employing the first 15 well-resolved reflections (located using the derivative-based peak search algorithm provided with Fullprof.2k),[25] a fixed absolute error on each line of 0.03° 2θ, and a tolerance of two impurity lines. Initial unit cell metrics in the monoclinic crystal system were calculated with reasonable figures-of-merit: $M(13)^{26a} = 16.7$ and $F(13)^{26b} = 36.1$. Systematic absences were examined using the software package CHECKCELL,[27] and the space group $P2_1$ was unambiguously assigned as the most suitable to describe the symmetry of the material. Indeed, a Le Bail[21] whole-powder-diffraction-pattern profile decomposition in $P2_1$ produced a much better fit ($R_{Bragg} = 1.03\%$ and $\chi^2 = 9.85$; see Figure S2 in the Supporting Information) with the unit cell parameters ultimately converging to $a = 14.725(4)$ Å, $b = 26.194(8)$ Å, $c = 12.859(3)$ Å, and $\beta = 109.08(1)°$. As usually observed for this type of inclusion complexes,[8k,12e,19] the crystallinity is drastically reduced after inclusion due, essentially, to extensive structural disorder associated with both the host−guest system and the various water molecules of crystallization. This is clearly evident in the experimental diffractogram, which shows very low-resolved lines at low angle, and after approximately 30° 2θ, the signal is almost indiscernible from the noise.

Following the strategy previously described by us for the inclusion complex TRIMEB·$CpMo(CO)_3Cl$·$5H_2O$,[12e] the structural modeling of a hypothetical packing for the inclusion complex **3** using the software package FOX[28] assumes that (i) the interactions between the guest species, Cp_2NbCl_2, and the cyclodextrin host are essentially of weak nature (i.e., van der Waals and, eventually, some weak C−H···(Cl,O) hydrogen-bonding interactions); (ii) individual chemical moieties are distributed in order to fill the available space effectively; and (iii) the molecular geometry of each chemical moiety remains relatively unchanged after inclusion. The latter assumption is of critical importance because, in the absence of a detailed crystal structure determination (from single-crystal X-ray data) for a true inclusion complex, it means we can select from the literature a conformation for TRIMEB that better adjusts to the type of guest molecule we are employing in the present work. Thus, reported molecular geometries for the host and guest chemical entities (see following paragraphs) were employed in the global optimization process, with each molecule being added to the FOX code as mathematical objects in the form of Fenske−

(19) Petrovski, Z.; Braga, S. S.; Santos, A. M.; Rodrigues, S. S.; Gonçalves, I. S.; Pillinger, M.; Kühn, F. E.; Romão, C. C. *Inorg. Chim. Acta* **2005**, *358*, 981.

(20) Boultif, A.; Louer, D. *J. Appl. Crystallogr.* **2004**, *37*, 724.

(21) LeBail, A.; Duroy, H.; Fourquet, J. L. *Mater. Res. Bull.* **1988**, *23*, 447.

(22) (a) Allen, F. H. *Acta Crystallogr., Sect. B: Struct. Sci.* **2002**, *58*, 380. (b) Allen, F. H.; Motherwell, W. D. S. *Acta Crystallogr., Sect. B: Struct. Sci.* **2002**, *58*, 407.

(23) CSD refcodes of TRIMEB inclusion complexes: ASIQOI, ASIQUO, AZOYOD, BIFGIH, BIFGON, BIFGUT, CAMPIP, CAMPIP10, COYXAP, COYXAP10, COYXET, COYXET10, COYXET20, EKOGOA, EKOGUG, EZAVOQ, FEXBUG, GELKEN, GELKEN10, HEZWAK, HEZWAK01, MODHUI, NIZHAF, PAFSOE, PINMAA, QOYLIZ, RONWOG, WAGLOG, WAGLUM, XAQJII, XAQJII01, ZIFQOU.

(24) CSD refcodes of monoclinic TRIMEB inclusion complexes: ASIQOI, ASIQUO, BIFGON, EKOGUG, EZAVOQ, FEXBUG.

(25) (a) Rodriguez-Carvajal, J. *FULLPROF−A Program for Rietveld Refinement and Pattern Matching Analysis, Abstract of the Satellite Meeting on Powder Diffraction of the XV Congress of the IUCR*; Toulouse, France, 1990; p 127. (b) Roisnel, T.; Rodriguez-Carvajal, J. *WinPLOTR [June 2005]−A Windows Tool for Powder Diffraction Pattern Analysis, Proceedings of the Seventh European Powder Diffraction Conference (EPDIC 7), Mater. Sci. Forum* **2001**, *378−381*, 118−123.

(26) (a) Boultif, A.; Louer, D. *J. Appl. Crystallogr.* **1991**, *24*, 987. (b) Louer, D. In *Automatic Indexing: Procedures and Applications, Accuracy in Powder Diffraction II*; Gaithersburg, MD, 1992; pp 92−104.

(27) Laugier, J.; Bochu, B. CHECKCELL−*A Software Performing Automatic Cell/Space Group Determination, Collaborative Computational Project Number 14 (CCP14)*; Laboratoire des Matériaux et du Génie Physique de l'Ecole Supérieure de Physique de Grenoble (INPG): France, 2000.

(28) (a) Favre-Nicolin, V.; Cerný, R. *J. Appl. Crystallogr.* **2002**, *35*, 734. (b) Favre-Nicolin, V.; Cerný, R. *FOX−A Program for ab Initio Structure Solution from Powder Diffraction Data*, Program Developed for the Swiss National Science Foundation; University of Geneva: Geneva, Switzerland, 2000.

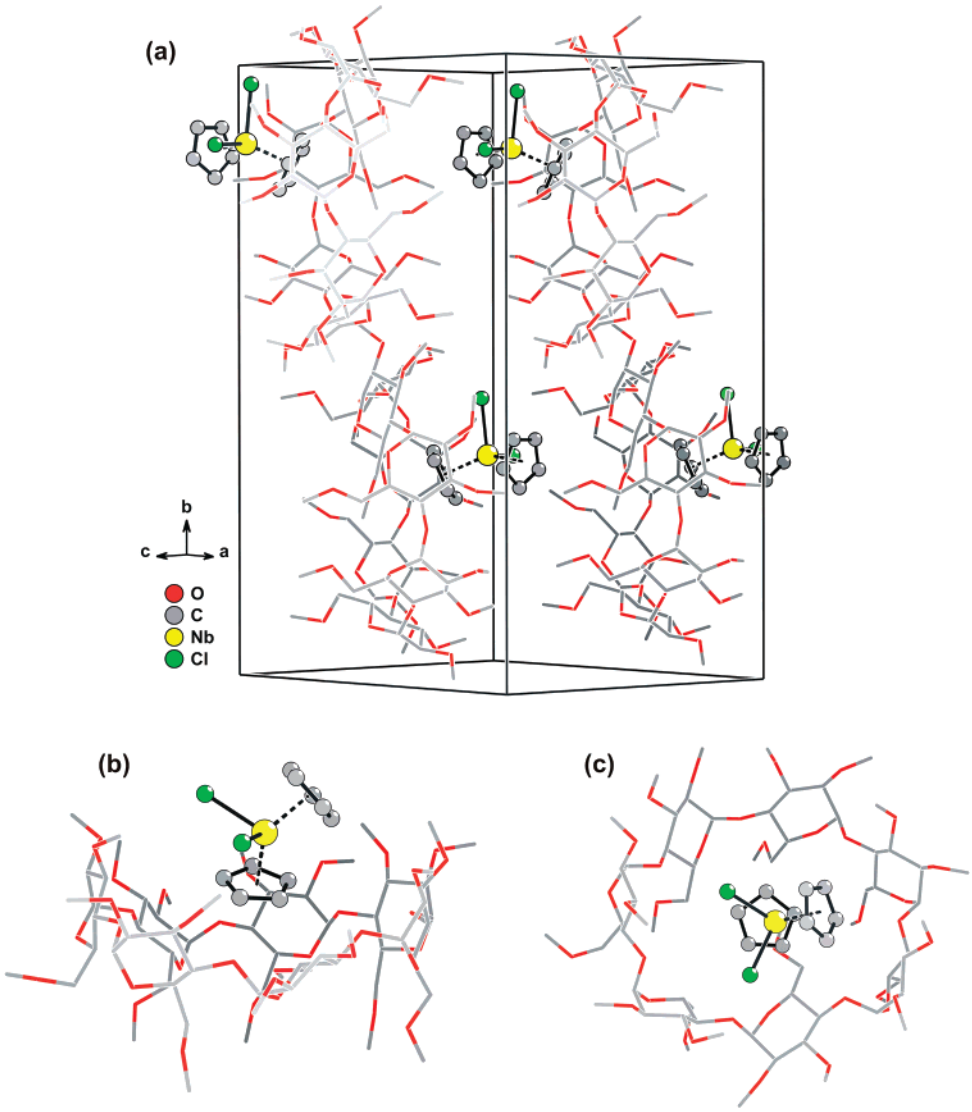

Figure 2. (a) Unit cell contents of the hypothetical structural model of the inclusion complex comprising TRIMEB and Cp_2NbCl_2. (b and c) Detailed perspective views of the inclusion complex. Nb−C bonds to the η^5-Cp rings have been omitted for clarity and replaced by a black-filled dashed bond to the respective centroid.

Hall Z-matrices created using BABEL (hydrogen atoms have been removed in order to simplify the calculations).[29]

Atomic coordinates of Cp_2NbCl_2 were taken from the structure reported by Prout et al.[30] (CSD refcode CPCLNB), with the pivot atom of the Z-matrix being the central Nb such that the mobility of the rigid chemical entity within the unit cell was greatly facilitated. In the structure described by Prout et al., Z′ is equal to 2, with each one of the crystallographically independent molecules showing a distinct type of conformation: while one has the two Cp rings eclipsed, the other has them staggered. For the calculations carried out in the present work, only the staggered conformation was used, based on the assumption that in the absence of other identical moieties nearby the molecule should adopt the conformation with the lowest energy when included in TRIMEB. For the cyclodextrin TRIMEB, among the six known monoclinic structures,[24] attempts at a global optimization with the geometries reported by Tsorteki et al.[31] (CSD refcode ASIQUO) and Caira et al.[32] (CSD refcode BIFGON) failed to produce chemically feasible structural models. Indeed, Monte Carlo optimizations launched in FOX (using the optimized parallel tempering algorithm), with the individual mathematical objects starting in random crystallographic positions, systematically led to either true noninclusion complexes, in which the Cp_2NbCl_2 molecule was located outside the toroidal cavity of TRIMEB, or, more frequently, the organometallic species was instead located "on top" of some glucose residues of TRIMEB. This latter and rather frequent occurrence in the optimization led us to conclude that, most likely, in order to isolate a true inclusion complex, TRIMEB should be significantly distorted so that the Cp_2NbCl_2 molecule could easily be accommodated within the cavity. A search in the literature revealed that Caira and collaborators recently reported a new crystalline form of TRIMEB, in which a significant deviation from the toroidal symmetry leads to a distinct elliptical cavity (CSD refcode WAGLUM).[33] Therefore, a Monte Carlo optimization (using the optimized parallel

(29) Walters, P.; Stahl, M. *BABEL Version 1.3−A Program for the Interconversion of File Formats Used in Molecular Modelling*; Department of Chemistry, University of Arizona: Tucson, AZ, 1996.

(30) Prout, K.; Cameron, T. S.; Forder, R. A. *Acta Crystallogr., Sect. B: Struct. Sci.* **1974**, *30*, 2290.

(31) Tsorteki, F.; Bethanis, K.; Mentzafos, D. *Carbohydr. Res.* **2004**, *339*, 233.

(32) Caira, M. R.; Hunter, R.; Bourne, S. A.; Smith, V. J. *Supramol. Chem.* **2004**, *16*, 395.

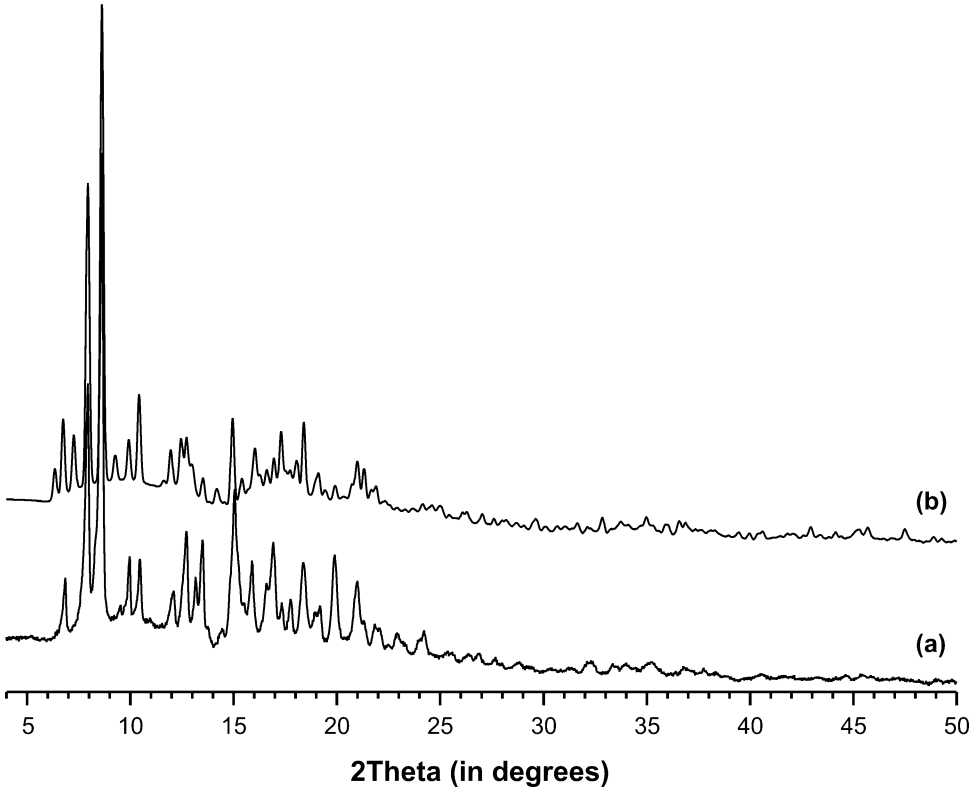

Figure 3. Powder X-ray diffraction patterns of (a) as-synthesized TRIMEB inclusion complex **3** and (b) hypothetical structural model for the inclusion complex comprising TRIMEB and Cp_2NbCl_2.

tempering algorithm), having the parameters of the Z-matrices of CPCLNB and WAGLUM fixed (i.e., the individual molecular entities were treated as rigid bodies), was launched in FOX. As the powder XRD data are also affected by textural effects, such as preferred orientation, a refineable March−Dollase correction was also included in the optimization.[34] After Monte Carlo optimization without the need to apply antibump restraints and ignoring the presence of water molecules of crystallization, the structural model converged to that depicted in Figure 2, which fully supports the existence of a true inclusion complex. Fractional atomic coordinates for the hypothetical structural model are supplied as Supporting Information. A comparison between the experimental powder XRD pattern and a simulation for the hypothetical unit cell (Figure 2) is provided in Figure 3 (calculated weighted residual of $R_{wp} = 0.168$). It is important to emphasize that when started from distinct random initial locations, the optimization with FOX produced nearly the same final crystallographic positions for both the host and the guest molecules and with comparable *R* factors.

As previously encountered for the inclusion complex TRIMEB·$CpMo(CO)_3Cl·5H_2O$,[12e] the quality of the experimental powder XRD pattern for TRIMEB·$Cp_2NbCl_2·4H_2O$ (**3**) prevents a successful unrestrained Rietveld refinement of the structural model using, for example, FULLPROF[25a] routines. Such an attempt will probably be possible only using high-resolution data from a synchrotron X-ray source.

The $^{13}C\{^1H\}$ CP/MAS NMR spectra of Cp_2NbCl_2 (**1**), native β-CD, TRIMEB, and the two inclusion complexes are shown in Figure 4. Native β-CD hydrate exhibits a complex spectrum, with multiple sharp resonances for each type of carbon atom. These features have been correlated with different torsion angles about the $\alpha(1\rightarrow4)$ linkages[35a,b] and with torsion angles describing the orientation of the hydroxyl groups.[35c] Upon inclusion to give complex **2**, the resonances due to the C1, C4, C2,3,5, and C6 host carbon atoms appear mainly as single broad peaks centered around 103, 82, 73, and 61 ppm, respectively. These changes are typically attributed to a symmetrization of the β-CD macrocycle; that is, the encapsulation of the guest molecule induces the ring to adopt a less distorted conformation, with each glucose unit in a more similar environment.[12e,36] The low crystallinity of complex **2** and the presence of paramagnetic Nb^{IV} guest species may also contribute to the broadening of the peaks. The $^{13}C\{^1H\}$ CP/MAS NMR spectrum of complex **2** contains an additional low-intensity peak at about 115 ppm, attributed to the Cp carbon atoms of the guest molecule, which is shifted slightly upfield with respect to the broad resonance observed for Cp_2NbCl_2 (**1**) (Figure 4).

Like native β-CD hydrate, the $^{13}C\{^1H\}$ CP/MAS NMR spectrum of TRIMEB also shows multiple resonances for each type of carbon atom (Figure 4). This is because the host assumes a severely collapsed conformation in the solid state, which minimizes the hydrophobic cavity in the absence of a hydrophobic guest.[37] By reference to the reported solution spectra,[38] the different carbon resonances are assigned to C1 (93−102 ppm), C2,3,4 (74−88 ppm), C5,6 (68−73 ppm), and O−Me

(33) Caira, M. R.; Bourne, S. A.; Mhlongo, W. T.; Dean, P. M. *Chem. Commun.* **2004**, 2216.

(34) (a) March, A. *Z. Kristallogr.* **1932**, *81*, 285. (b) Dollase, W. A. *J. Appl. Crystallogr.* **1986**, *19*, 267.

(35) (a) Gidley, M. J.; Bociek, S. M. *J. Am. Chem. Soc.* **1988**, *110*, 3820. (b) Heyes, S. J.; Clayden, N. J.; Dobson, C. M. *Carbohydr. Res.* **1992**, *233*, 1. (c) Veregin, R. P.; Fyfe, C. A.; Marchessault, R. H.; Tayler, M. G. *Carbohydr. Res.* **1987**, *160*, 41.

(36) Cunha-Silva, L.; Teixeira-Dias, J. J. C. *New J. Chem.* **2005**, *29*, 1335.

(37) Brown, G. R.; Caira, M. R.; Nassimbeni, L. R.; van Oudtshoorn, B. *J. Inclusion Phenom. Macrocyclic Chem.* **1996**, *26*, 281.

(38) (a) Johnson, J. R.; Shankland, N.; Sadler, I. H. *Tetrahedron* **1985**, *41*, 3147. (b) Yamamoto, Y.; Onda, M.; Takahashi, Y.; Inoue, Y.; Chûjô, R. *Carbohydr. Res.* **1987**, *170*, 229.

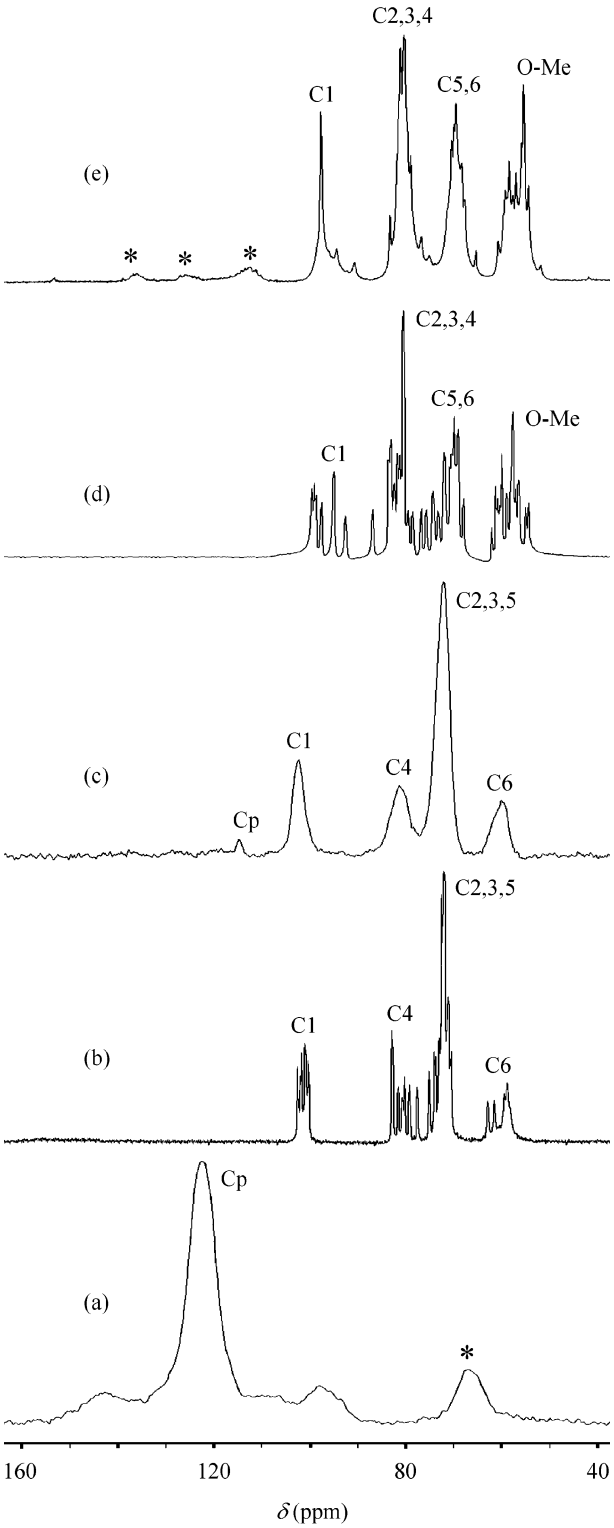

Figure 4. Solid-state $^{13}C\{^1H\}$ CP/MAS NMR spectra of (a) Cp_2NbCl_2 (**1**), (b) native β-CD hydrate, (c) the β-CD inclusion complex **2**, (d) TRIMEB, and (e) the TRIMEB inclusion complex **3**. Asterisks denote spinning sidebands.

(54−64 ppm). Several resolved lines are also observed for the inclusion complex **3**, which is consistent with the relatively high crystallinity of the complex revealed by powder XRD. A comparison of the spectra for TRIMEB and complex **3** reveals considerable differences in the number, relative intensities, and positions of peaks due to the host, which indicates that the conformation of the macrocycle is different in the two samples. The presence of at least nine sharp lines for the methyl carbon

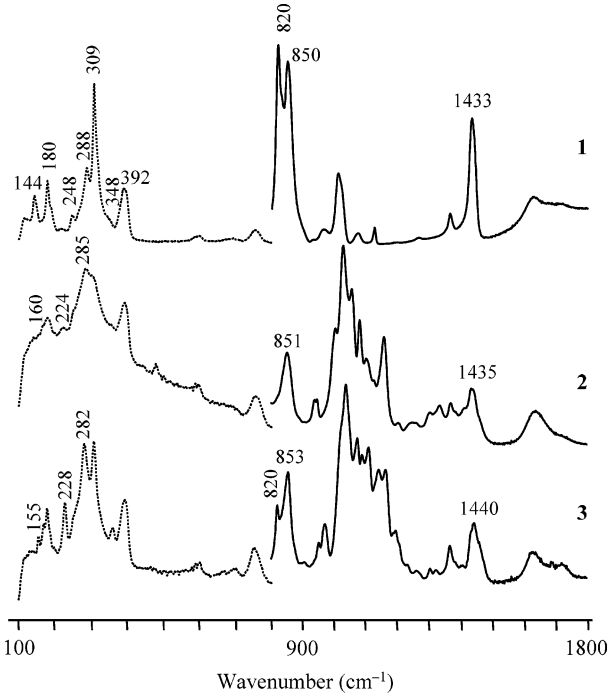

Figure 5. Raman (dashed lines) and FTIR (solid lines) spectra of Cp_2NbCl_2 (**1**), the β-CD inclusion complex **2**, and the TRIMEB inclusion complex **3** in the 100−1800 cm^{-1} region.

Table 1. Experimental Raman Wavenumbers (cm^{-1}) for Cp_2NbCl_2 (1), the β-CD Inclusion Complex 2, and the TRIMEB Inclusion Complex 3 in the 100−400 cm^{-1} Range (approximate descriptions for the observed bands of 1 are also included)

calculated[a]	Raman			
1	**1**	**2**	**3**	approximate description[b]
139	144	160	155	δ(Cp−Nb−Cp)
160	180	180	180	δ(Cl−Nb−Cl)
243	248	224	228	ν_{as}(Nb−Cl)
248	288	285	282	ν_{s}(Nb−Cl)
276	309	309	309	ν_{s}(Nb−Cp)
331	348	348	348	*t*(Cp)
337	392	392	392	ν_{as}(Nb−Cp)

[a] Scaled values (scale factor = 0.961). [b] ν = stretching, δ = bending, *t* = tilting.

atoms shows that these groups exist in several different well-defined environments. With respect to the guest species, resonances for the Cp groups cannot be discerned.

Figure 5 shows the Raman and FTIR spectra of compounds Cp_2NbCl_2 (**1**), β-CD·Cp_2NbCl_2·$10H_2O$ (**2**), and TRIMEB·Cp_2NbCl_2·$4H_2O$ (**3**) in the region 100−1800 cm^{-1}. The spectra for the two inclusion complexes contain several bands that are coincident with the typical bands exhibited by pure β-CD and TRIMEB, suggesting that the hosts are not chemically modified upon interaction with Cp_2NbCl_2. Concerning the organometallic guest, a few changes can be observed in the spectra of the inclusion complexes relative to the pure compound **1**. These changes occur mainly in the bands at 820 and 1433 cm^{-1} (Figure 5). According to the ab initio calculations performed for compound **1**, the band at 820 cm^{-1} can be ascribed to the out-of-plane deformation modes of the C−H group (γC−H), while the band at 1433 cm^{-1} is assigned to the symmetric stretching of the C−C bonds in the cyclopentadienyl ring (νC−C). These assignments are in good agreement with those reported for

(39) Holubová, J.; Černošek, Z.; Pavlík, I. *Vib. Spectrosc.* **1997**, *14*, 147.

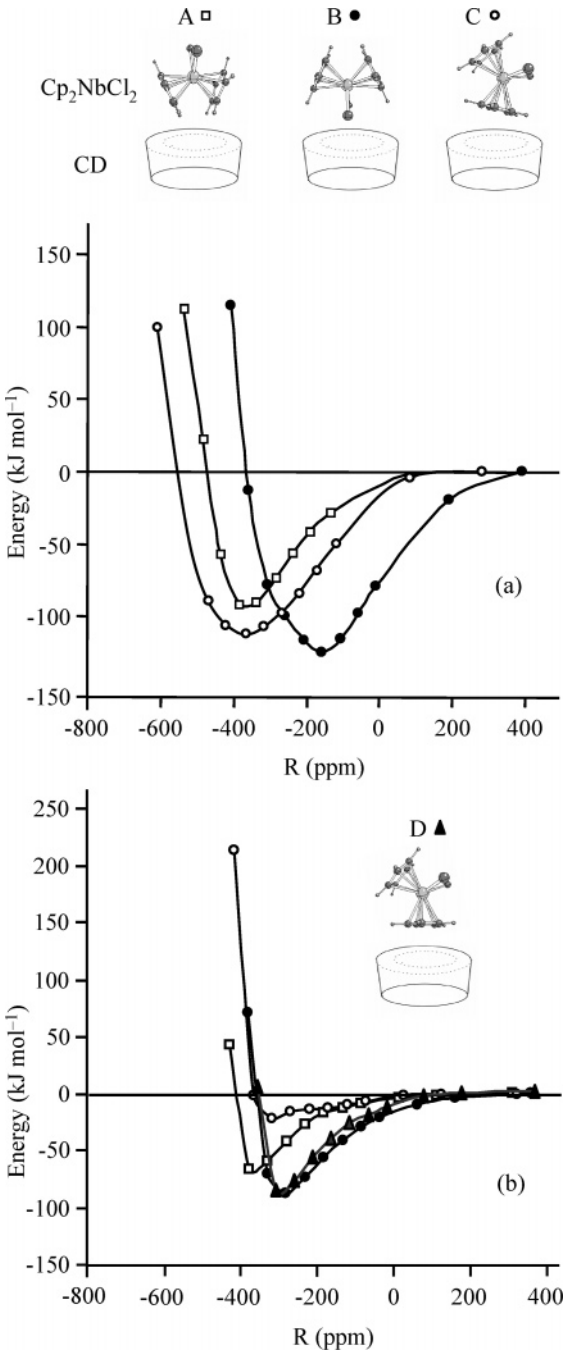

Figure 6. Plot of energy versus host−guest distance for the different β-CD−Cp_2NbCl_2 (a) and TRIMEB−Cp_2NbCl_2 (b) inclusion geometries. Structures A and B allow the inclusion of both cyclopentadienyl ligands, while structures C and D allow only one Cp inside the cavity. R is defined as the distance between the plane of the outer hydrogen atoms in the secondary hydroxyl or methoxy groups of the host and the nearest hydrogen atom of the approaching Cp_2NbCl_2 molecule. Negative R values refer to inclusion.

Cp_2NbCl_2.[39] The 820 cm^{-1} band appears with weak intensity for complex **3** and is totally absent for complex **2**, while the other γC−H band at 850 cm^{-1} is essentially unaffected. The behavior of the band at 820 cm^{-1} can be associated with the host−guest interaction and suggests that the interaction is stronger in complex **2** than in **3**. The 1433 cm^{-1} band is blue-shifted to 1435 cm^{-1} for **2** and 1440 cm^{-1} for **3**.

Table 1 gives the frequency values and approximate descriptions of the bands observed in the 100−400 cm^{-1} region. This is the frequency range of the metal−ligand vibrations (niobium−chlorine and niobium−cyclopentadienyl ring), where significant differences are expected due to the effect of the inclusion process. While the ν(Nb−Cp) mode is found to be insensitive to the inclusion process, the ν_{as}(Nb−Cl) mode is red-shifted from **1** to **2** and **3** by about 20 cm^{-1}. In contrast, the bending of the Cp−Nb−Cp presents blue-shifts of about 16 cm^{-1} from **1** to **2** and 11 cm^{-1} from **1** to **3**.

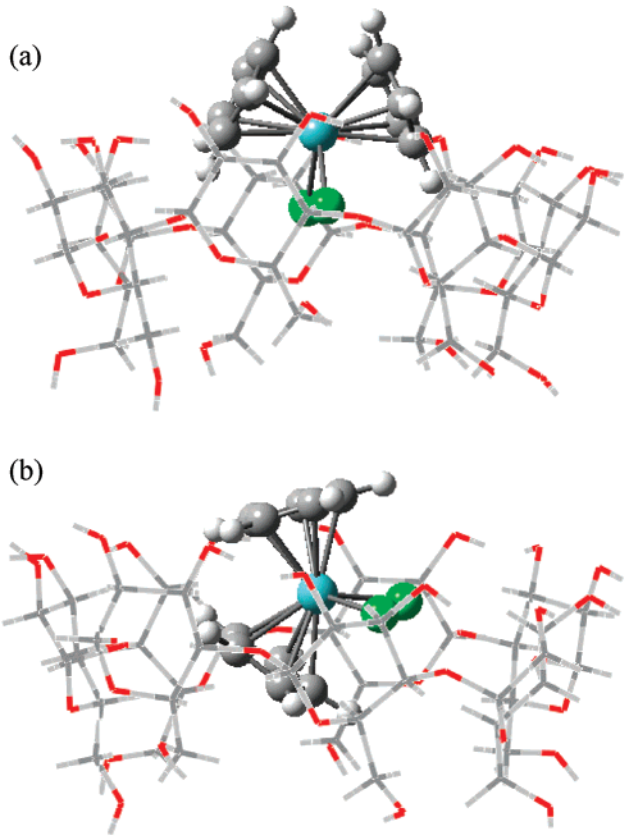

Figure 7. Schematic representation of the lowest energy inclusion geometries for the inclusion complex comprising β-CD and Cp_2NbCl_2.

The cyclodextrin−organometallic inclusion geometries were investigated by ab initio calculations, using a rigid-body approach. This approach does not account for the CD nonrigidity, but has been shown to give valuable clues concerning preferential inclusion geometries and guest mobility.[8k,l] Several different inclusion geometries were calculated with native β-CD and TRIMEB as the hosts in order to obtain the possible interaction geometries. Figure 6a shows the results obtained for three representative inclusion geometries for β-CD and Cp_2NbCl_2. Structures A and B allow the inclusion of both Cp ligands, while structure C allows only one Cp inside the cyclodextrin cavity. The reliability of the inclusion geometries obtained at different computational levels has recently been assessed by Casadesús et al.,[40] based on the occurrence of unrealistic H···H host−guest contacts. Structures A and B with β-CD as the host present only two H···H contacts in the 165−200 pm range, while none are present for structure C. As noted by Casadesús et al.,[40] a small number of short contacts are acceptable and the values below 200 pm are not necessarily unphysical. Thus we may assume that the calculated structures are plausible, despite the well-known limitations of this approach. The energy profiles obtained for the inclusion of Cp_2-

(40) Casadesús, R.; Moreno, M.; González-Lafont, À.; Lluch, J. M.; Repasky, M. P. *J. Comput. Chem.* **2004**, *25*, 99.

$NbCl_2$ in β-CD show that the energy differences between the minima are small (Figure 6a). Thus it is likely that all three structures compete at room temperature and the orientation of the Cp_2NbCl_2 molecule inside the cavity will be able to vary easily. The lowest energy structure for this inclusion complex was found to be structure B, with a shallow inclusion of both of the Cp ligands (Figure 7a), while a deep inclusion is obtained with structure C (Figure 7b). These results suggest that a 1:1 host:guest ratio would be favored by structure C and a 2:1 ratio by structures A and B. In both cases, it is expected that the inclusion process will promote the observed changes in the vibrations of the Nb−Cl bonds, as discussed above.

Figure 6b presents the energy profile obtained for TRIMEB−Cp_2NbCl_2 inclusion geometries. In addition to structures A, B, and C, the results obtained for the inclusion geometry present in the structural model derived from powder XRD (labeled D) are also shown. Structure D is clearly plausible, with an inclusion energy curve nearly coincident with that for the lowest energy structure B. However, the energy differences between the A, B, and D minima are small, allowing the organometallic compound to keep some orientational freedom inside the TRIMEB cavity.

Conclusions

Among the cyclodextrin−organometallic inclusion complexes described in the literature, only a few have been successfully characterized by single-crystal X-ray diffraction, mainly because of the difficulty in preparing crystals of appropriate size that exhibit stability under the X-ray beam over the period of data collection. Useful structural information can, however, be obtained through a combination of other techniques such as powder XRD and NMR spectroscopy. In the present work we have shown that niobocene dichloride, Cp_2NbCl_2, forms inclusion complexes with native β-cyclodextrin (β-CD) and permethylated β-CD (TRIMEB). The TRIMEB adduct is sufficiently crystalline to allow indexing of the powder XRD pattern and structural modeling of a hypothetical crystal packing. Ab initio calculations fully support the plausibility of the host−guest inclusion geometry arrived at in the structural model. In future work, the potential antiproliferative and cytotoxic activities of Cp_2NbCl_2 and its cyclodextrin inclusion complexes will be studied and a comparison made with the results already obtained with the molybdenocene analogue, Cp_2MoCl_2.

Experimental Section

General Comments. All air-sensitive operations were carried out using standard Schlenk techniques under nitrogen. β-CD hydrate was kindly donated by Laboratoires La Roquette (France), and heptakis-2,3,6-tri-*O*-methyl-β-CD was obtained from Fluka. Cp_2NbCl_2 (**1**) was prepared according to the literature procedure.[41]

Microanalyses for CHN were performed at the ITQB, Oeiras, Portugal (by C. Almeida). TGA studies were performed using a Shimadzu TGA-50 system at a heating rate of 5 K min^{-1} under a static atmosphere of air. The room-temperature FT-Raman spectra were recorded on a RFS-100 Bruker FT spectrometer, in the 70−4000 cm^{-1} range, using a Nd:YAG laser (Coherent Compass-1064/500) with an excitation wavelength of 1064 nm and a resolution of 2 cm^{-1}. Room-temperature FTIR spectra were recorded on a Mattson 7000 FTIR spectrometer, in the 300−4000 cm^{-1} range, using a globar source, a DTGS detector, and potassium bromide cells, with 2 cm^{-1} resolution and triangular apodization. $^{13}C\{^1H\}$ CP/MAS NMR spectra were recorded at 125.72 MHz on a (11.7 T) Bruker Avance 500 spectrometer, with an optimized π/2 pulse for ^1H of 4.5 μs, 2 ms contact time, a spinning rate of 7 kHz, and 12 s recycle delays. Chemical shifts are quoted in parts per million from tetramethylsilane.

Powder X-ray diffraction data were collected at ambient temperature on a X'Pert MPD Philips diffractometer (Cu Kα, λ = 1.54060 Å), equipped with an X'Celerator detector, curved graphite-monochromated radiation, and a flat-plate sample holder, in a Bragg−Brentano para-focusing optics configuration (40 kV, 50 mA). Intensity data were collected in continuous scanning mode in the ca. $3° \le 2\theta \le 70°$ angular range. XRD data for air-sensitive Cp_2NbCl_2 were collected with the same working conditions but under a low pressure of ca. 0.1 mbar.

β-CD·Cp_2NbCl_2·$10H_2O$ (2). A solution of β-CD hydrate (0.45 g, 0.34 mmol) in water was added dropwise to a cold solution of Cp_2NbCl_2 (**1**) (0.10 g, 0.34 mmol) in dry ethanol. The mixture was stirred at 0 °C under nitrogen for 20 min and then evaporated to dryness under reduced pressure to obtain a pale yellow solid. Anal. Calcd for $(C_{42}H_{70}O_{35})\cdot(C_{10}H_{10}NbCl_2)\cdot 10H_2O$ (1609.1): C 38.81, H 6.26. Found: C 39.16, H 6.59. TGA up to 130 °C revealed a sample weight loss of 12.0% (calcd for loss of $10H_2O$, 11.2%). FTIR (KBr, cm^{-1}): 3358 vs, 3103 w, 2927 m, 1637 m, 1435 m, 1412 sh, 1369 m, 1334 m, 1301 w, 1248 vw, 1204 vw, 1158 s, 1127 sh, 1107 vw, 1080 m, 1056 sh, 1029 vs, 1004 sh, 947 w, 937 w, 851 m, 753 m, 705 w, 658 vw, 610 sh, 577 m, 529 w, 480 vw, 442 vw. $^{13}C\{^1H\}$ CP/MAS NMR: δ 115.3 (guest, Cp), 103.0 (β-CD, C1), 82.0 (β-CD, C4), 72.9 (β-CD, C2,3,5), 60.8 (β-CD, C6).

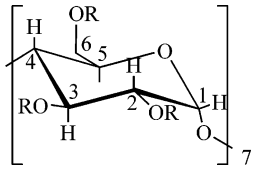

Figure 8. Carbon atom numbering scheme for β-CD (R = H) and TRIMEB (R = Me).

TRIMEB·Cp_2NbCl_2·$4H_2O$ (3). A solution of TRIMEB (0.59 g, 0.41 mmol) in undried, degassed dichloromethane was added dropwise to a cold solution of Cp_2NbCl_2 (120 mg, 0.41 mmol) in dry ethanol. After stirring at 0 °C under inert atmosphere for 20 min, the solution was evaporated to dryness under reduced pressure to give a pale greenish-yellow solid. Anal. Calcd for $(C_{63}H_{112}O_{35})\cdot(C_{10}H_{10}NbCl_2)\cdot 4H_2O$ (1795.6): C 48.83, H 7.30. Found: C 48.73, H 6.92. TGA up to 95 °C revealed a sample weight loss of 4.0% (calcd for loss of $4H_2O$, 4.0%). FTIR (KBr, cm^{-1}): 3415 vs, 3100 m, 2977 m, 2927 m, 2833 m, 1630 m, 1440 m, 1367 m, 1321 vw, 1303 vw, 1193 sh, 1164 m, 1139 m, 1112 sh, 1108 m, 1087 w, 1072 m, 1037 s, 1021 sh, 970 w, 952 vw, 853 m, 820 w, 753 m, 703 vw, 653 w, 578 m, 552 sh. $^{13}C\{^1H\}$ CP/MAS NMR: δ 99.9, 96.7, 92.9 (TRIMEB, C1), 83.3, 82.5, 81.2, 78.9, 77.4 (TRIMEB, C2,3,4),

(41) Curtis, M. D.; Bell, L. G.; Butler, W. M. *Organometallics* **1985**, *4*, 701.

(42) Frisch, M. J.; Trucks, G. W.; Schlegel, H. B.; Scuseria, G. E.; Robb, M. A.; Cheeseman, J. R.; Montgomery, J. A., Jr.; Vreven, T.; Kudin, K. N.; Burant, J. C.; Millam, J. M.; Iyengar, S. S.; Tomasi, J.; Barone, V.; Mennucci, B.; Cossi, M.; Scalmani, G.; Rega, N.; Petersson, G. A.; Nakatsuji, H.; Hada, M.; Ehara, M.; Toyota, K.; Fukuda, R.; Hasegawa, J.; Ishida, M.; Nakajima, T.; Honda, Y.; Kitao, O.; Nakai, H.; Klene, M.; Li, X.; Knox, J. E.; Hratchian, H. P.; Cross, J. B.; Adamo, C.; Jaramillo, J.; Gomperts, R.; Stratmann, R. E.; Yazyev, O.; Austin, A. J.; Cammi, R.; Pomelli, C.; Ochterski, J. W.; Ayala, P. Y.; Morokuma, K.; Voth, G. A.; Salvador, P.; Dannenberg, J. J.; Zakrzewski, V. G.; Dapprich, S.; Daniels, A. D.; Strain, M. C.; Farkas, O.; Malick, D. K.; Rabuck, A. D.; Raghavachari, K.; Foresman, J. B.; Ortiz, J. V.; Cui, Q.; Baboul, A. G.; Clifford, S.; Cioslowski, J.; Stefanov, B. B.; Liu, G.; Liashenko, A.; Piskorz, P.; Komaromi, I.; Martin, R. L.; Fox, D. J.; Keith, T.; Al-Laham, M. A.; Peng, C. Y.; Nanayakkara, A.; Challacombe, M.; Gill, P. M. W.; Johnson, B.; Chen, W.; Wong, M. W.; Gonzalez, C.; Pople, J. A. *GAUSSIAN 03*, Revision B.04; Gaussian, Inc.: Pittsburgh, PA, 2003.

72.6, 72.1, 71.7, 70.5, 69.9, 67.5 (TRIMEB, C5,6), 63.1, 61.6, 60.7, 60.0, 59.4, 58.2, 57.8, 56.8, 54.2 (TRIMEB, O-CH_3).

Computational Details. Ab initio calculations were performed using the G03W program package running on a personal computer.[42] The fully optimized geometry and the harmonic vibrational frequencies for the free organometallic Cp_2NbCl_2 (**1**) were obtained at the B3LYP level, using the standard LanL2DZ basis set and effective core potentials.[43] For the comparison with the experimental values, the calculated wavenumbers were scaled by a factor of 0.961.[44] In order to obtain the best cyclodextrin−organometallic interaction geometries for β-CD−Cp_2NbCl_2 and TRIMEB−Cp_2NbCl_2, several possible inclusion geometries were calculated by a set of single-point calculations at the HF level with the Stevens/Basch/Krauss effective core potentials minimal basis.[45] The geometry of the β-CD host was taken from the most suitable X-ray structure available,[46] while for TRIMEB the geometry used to obtain the final structural model from powder XRD was used (see Figure 2).

Acknowledgment. We are grateful to the FCT, POCI 2010, OE, and FEDER for funding (Project POCI/CTM/58507/2004). We also wish to acknowledge Paula Esculcas for assistance in the NMR experiments, Rosário Soares and Luis Silva for collecting the powder X-ray diffraction patterns, and Professor Armando Duarte for access to TGA equipment.

Supporting Information Available: Experimental data, Le Bail whole-powder-diffraction-pattern profile fitting and difference powder XRD patterns for the inclusion complex TRIMEB·Cp_2NbCl_2·$4H_2O$ (**3**), and fractional atomic coordinates for the final optimized structural model. This material is available free of charge via the Internet at http://pubs.acs.org.

OM7003749

(43) Wadt, W. R.; Hay, P. J. *J. Chem. Phys.* **1985**, *82*, 284.

(44) NIST Computational Chemistry Comparison and Benchmark Database, NIST Standard Reference Database Number 101, Release 12, Aug 2005, Johnson, R. D., III, Ed.; http://srdata.nist.gov/cccbdb.

(45) (a) Stevens, W. J.; Basch, H.; Krauss, M. *J. Chem. Phys.* **1984**, *81*, 6026. (b) Stevens, W. J.; Krauss, M.; Basch, H.; Jasien, P. G. *Can. J. Chem.* **1992**, *70*, 612.

(46) Braga, S. S.; Aree, T.; Imamura, K.; Vertut, P.; Boal-Palheiros, I.; Saenger, W.; Teixeira-Dias, J. J. C. *J. Inclusion Phenom. Macrocyclic Chem.* **2002**, *43*, 115.